2007

The role of the cytoplasmic pore in inward rectification of Kir2.1 channels

Harley T. Kurata
Washington University School of Medicine in St. Louis
Wayland W. Cheng
Washington University School of Medicine in St. Louis
Christine Arrabit
Peptide Biology Laboratory
Paul A. Slesinger
Peptide Biology Laboratory
Colin G. Nichols
Washington University School of Medicine in St. Louis

Published July 16, 2007

ARTICLE

The Role of the Cytoplasmic Pore in Inward Rectification of Kir2.1 Channels

Harley T. Kurata,[1] Wayland W. Cheng,[1] Christine Arrabit,[2] Paul A. Slesinger,[2] and Colin G. Nichols[1]

[1]Department of Cell Biology and Physiology, Washington University School of Medicine, St. Louis, MO 63110
[2]The Salk Institute for Biological Studies, Peptide Biology Laboratory, La Jolla, CA 92037

Steeply voltage-dependent block by intracellular polyamines underlies the strong inward rectification properties of Kir2.1 and other Kir channels. Mutagenesis studies have identified several negatively charged pore-lining residues (D172, E224, and E299, in Kir2.1) in the inner cavity and cytoplasmic domain as determinants of the properties of spermine block. Recent crystallographic determination of the structure of the cytoplasmic domains of Kir2.1 identified additional negatively charged residues (D255 and D259) that influence inward rectification. In this study, we have characterized the kinetic and steady-state properties of spermine block in WT Kir2.1 and in mutations of the D255 residue (D255E, A, K, R). Despite minimal effects on steady-state blockade by spermine, D255 mutations have profound effects on the blocking kinetics, with D255A marginally, and D255R dramatically, slowing the rate of block. In addition, these mutations result in the appearance of a sustained current (in the presence of spermine) at depolarized voltages. These features are reproduced with a kinetic model consisting of a single open state, two sequentially linked blocked states, and a slow spermine permeation step, with residue D255 influencing the spermine affinity and rate of entry into the shallow blocked state. The data highlight a "long-pore" effect in Kir channels, and emphasize the importance of considering blocker permeation when assessing the effects of mutations on apparent blocker affinity.

INTRODUCTION

Inwardly rectifying K^+ (Kir) channels exhibit the property of preferentially passing currents in the inward direction, a consequence of channel blockade by intracellular polyamines (spermine, spermidine, cadaverine, and putrescine) (Lopatin et al., 1994; Fakler et al., 1995). A range of rectification properties are exhibited by different members of the structural family of Kir channels, arising from differences in the sensitivity and voltage dependence of polyamine block (Nichols and Lopatin, 1997; Lu, 2004). The strongest inward rectifiers (e.g., Kir2.1) are blocked so potently by spermine that, at depolarized voltages, they conduct little or no outward current under physiological conditions.

Because of their critical importance in the maintenance of a stable resting membrane potential, and in the shaping of action potentials, many studies have aimed to elucidate the molecular mechanisms underlying polyamine block of Kir channels (Lopatin et al., 1995; Xie et al., 2002, 2004; Guo and Lu, 2003; Guo et al., 2003; Kurata et al., 2004, 2006). There is considerable evidence that spermine block of Kir2.1 occurs in at least two sequential steps (Lopatin et al., 1995; Shin and Lu, 2005). A weakly voltage-dependent "shallow" blocking step involves entry of spermine into the Kir2.1 pore. A more strongly voltage-dependent "deep" blocking step entails movement of spermine to its stable binding site. Each step is likely coupled to movement of one or more K^+ ions that contribute to their respective voltage dependences.

Mutagenesis studies of Kir channels, combined with recent crystallographic data (Nishida and MacKinnon, 2002; Kuo et al., 2003; Pegan et al., 2005), have identified a number of pore-lining residues as important determinants of spermine blockade (Fig. 1). In the inner cavity, the presence of the negatively charged "rectification controller" residue (D172 in Kir2.1) is critical for high affinity spermine blockade, and introduction of a negative charge at an equivalent position (or elsewhere in the inner cavity) in weakly rectifying Kir channels introduces high-affinity and steeply voltage-dependent block by spermine (Lu and MacKinnon, 1994; Wible et al., 1994; Shyng et al., 1997; Guo et al., 2003; Kurata et al., 2004). The rectification controller residue may interact with spermine in its deep blocked state, and blocker protection experiments have suggested that this stable binding site lies between the rectification controller and the selectivity filter (Fig. 1 A; Chang et al., 2003; Kurata et al., 2006). Neutralization of negatively charged residues that line the cytoplasmic pore of Kir channels can also significantly affect polyamine block. The most widely characterized of these are residues E224 and E299 in Kir2.1 (Yang et al., 1995; Kubo and Murata, 2001; Guo et al., 2003; Fujiwara and Kubo, 2006), but a recent crystallographic study identified two new acidic

Correspondence to C.G. Nichols: cnichols@cellbio.wustl.edu

Published July 16, 2007

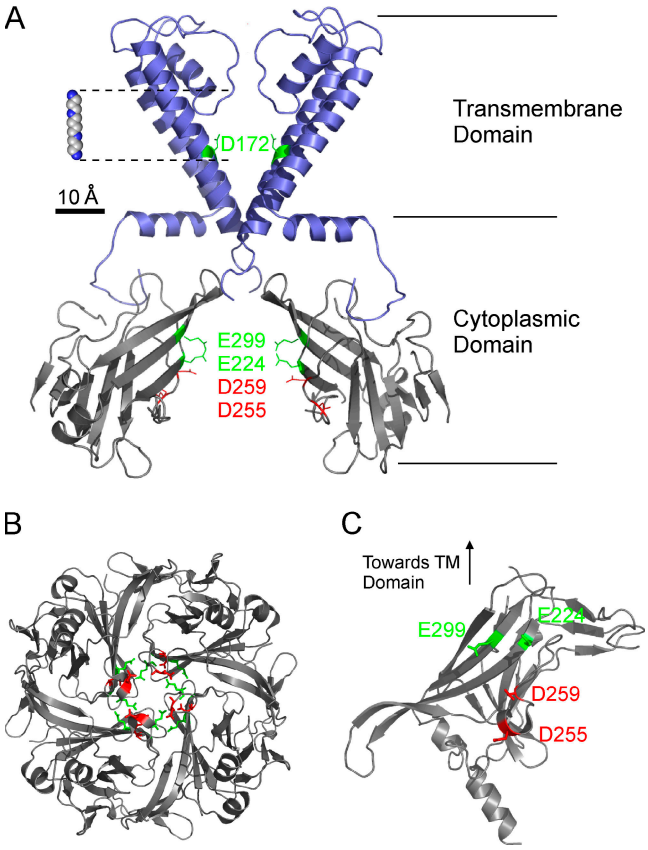

Figure 1. Locations of functionally important acidic residues in the pore of Kir2.1 channels, illustrated with the crystal structures of (A) KirBac1.1, and (B and C) the cytoplasmic domain of Kir2.1. Well-characterized residues (green) include the rectification controller residue (Kir2.1 D172) in the transmembrane domain, and Kir2.1 residues E224 and E299 in the cytoplasmic domain. Novel pore-lining aspartates in the Kir2.1 cytoplasmic domain (Pegan et al., 2005) are highlighted in red (D255 and D259). Spermine is shown to scale in A, in a position consistent with a deep binding site as identified by blocker protection studies (Chang et al., 2003; Kurata et al., 2006)

residues in Kir2.1 (D255 and D259) that also appear to be involved in determining inward rectification (Pegan et al., 2005). How these residues in the cytoplasmic domain contribute to the shallow or deep blocking steps is not completely understood. Interestingly, some studies suggest that electrostatic interactions between spermine and negatively charged residues in the cytoplasmic domain (shallow site) are critical for the stabilization of spermine in its deepest blocked state (Guo and Lu, 2003), while other studies have found that introduction of positive charges in the shallow site affect the transition to the deep blocked state but have little or no effect on spermine affinity of the deep blocked state (Kurata et al., 2004).

We postulated that negative charges at D255 would create electrostatic attraction for polyamines and, when mutated, would influence the affinity of polyamines in the shallow site. We investigated how multiple mutations

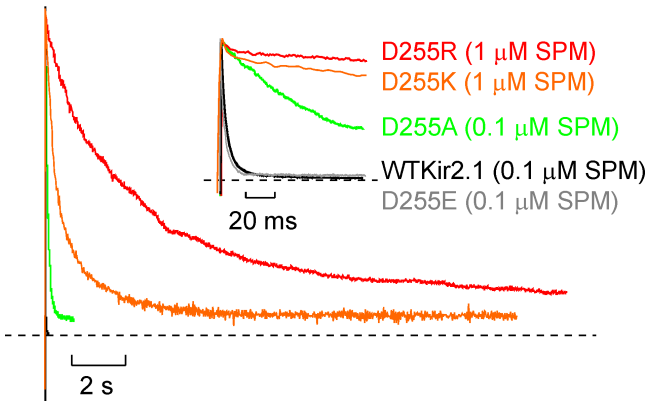

Figure 2. Kinetic role of acidic residues in the cytoplasmic domain of Kir2.1. Inside-out patches were excised from CosM6 cells expressing WT Kir2.1, Kir2.1 D255A, Kir2.1 D255E, Kir2.1 D255K, or Kir2.1 D255R. Normalized currents are shown at long and short (inset) time scales. From a holding potential of −80 mV, patches were pulsed to a voltage of +80 mV in the presence of 0.1 μM SPM (WT Kir2.1, D255A, D255E) or 1 μM SPM (D255K, D255R). Substitution of residue D255 with a neutral or basic amino acid does not abolish rectification but results in considerable deceleration of spermine block. (Inset) When currents are observed over shorter time scales sufficient to completely block WT Kir2.1 channels, the dramatic effects of D255 mutations (especially D255R) appear to result in complete abolition of any time-dependent block by spermine.

at D255 of Kir2.1 affect the kinetic and steady-state properties of spermine block. Mutations at this position have significant effects on the kinetics of channel block, and spermine affinity of the shallow blocked state, but have only indirect effects on spermine binding in its stable deep blocked state. Interestingly, D255R and D255K mutant channels revealed a pronounced plateau conductance at low spermine concentrations. A kinetic model that includes a step in which spermine slowly permeates the channel, from the deep binding site to the extracellular solution, can reproduce the features of Kir2.1 currents and the D255 mutant currents over a wide range of voltages and spermine concentrations.

MATERIALS AND METHODS

Kir2.1 Channel Constructs and Expression in COSm6 Cells

Point mutations (D255A, E, K, and R) in the WT mouse Kir2.1 (pcDNA3.1 vector) background were prepared using the Quikchange method (Stratagene). 2 d before recording, COSm6 cells were transfected with 1 μg of channel cDNA, using Fugene6 reagent. To efficiently identify transfected cells, channel cDNA was cotransfected with 300 ng of GFP cDNA (pGreenLantern; Invitrogen), allowing visualization of transfected cells using a standard epifluorescence attachment. Cells were maintained throughout in DMEM supplemented with 10% FBS, at 37°C in an air/5%CO_2 incubator.

Electrophysiological Experiments

Patch-clamp recordings were made at room temperature, in a chamber that allowed the solution bathing the exposed surface of the isolated patch to be changed rapidly. Data were normally

Published July 16, 2007

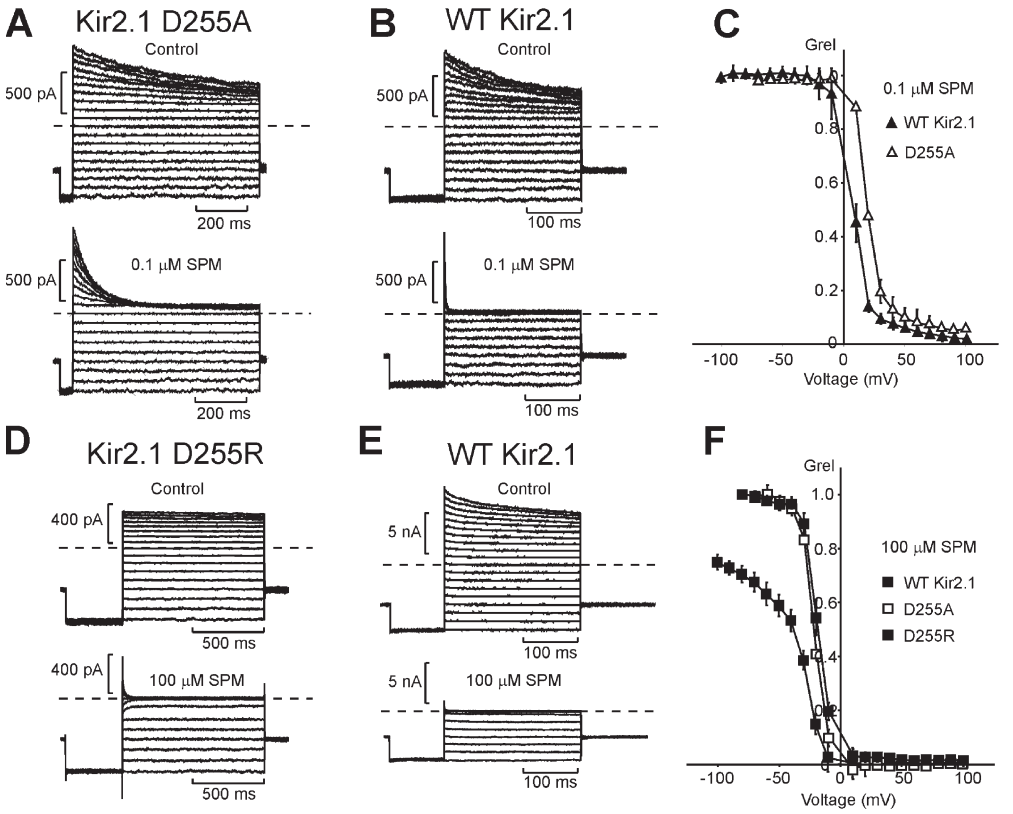

Figure 3. Steady-state features of spermine blockade of WT Kir2.1 and D255 mutant channels. (A and B) Inside-out patches expressing Kir2.1 D255A (A) or WT Kir2.1 (B) channels were pulsed in 10-mV increments from −80 to +100 mV, with 0.1 μM spermine in the intracellular bathing solution. (C) Steady-state currents in the presence of blocker, normalized to control (Grel) versus voltage. (D and E) Representative currents from similar voltage clamp experiments are shown for patches expressing WT Kir2.1 or Kir2.1 D255R channels in control and in the presence of 100 μM spermine. (F) Steady-state currents in the presence of blocker, normalized to control (Grel) versus voltage, for WT Kir2.1, D255A, and D255R channels in 100 μM spermine.

filtered at 2 kHz, signals were digitized at 5 kHz and stored directly on computer hard drive using Clampex software (Axon Inc.), though faster filtering and sampling were used for measurement of rapid channel kinetics. The standard pipette (extracellular) and bath (cytoplasmic) solution used in these experiments had the following composition: 140 mM KCl, 1 mM K-EGTA, 1 mM K-EDTA, 4 mM K_2HPO_4, pH 7. To accurately determine leak currents and capacitative transients, protocols were repeated in pH 5.0 solutions. The pH 5.0 condition was sufficient to abolish any detectable currents through Kir2.1 channels, and off-line subtraction of pH 5 currents was used for subsequent fitting of the kinetics of spermine block. Spermine was purchased from FLUKA-AG.

Modeling

Steady-state predictions of the kinetic model of spermine block were calculated in Microsoft Excel, after deriving an algebraic solution for steady-state occupancy of each state. The three-state model of spermine block was fitted to experimental G_{rel}-V curves, using the Microsoft Solver algorithm in Microsoft Excel. Fitted rate constants (0 mV) and effective valences for WT Kir2.1, D255A, and D255R channels are presented in Table I. For the purpose of model fitting, effective valences of transitions in the D255 mutants were assumed to be identical to those observed in the WT Kir2.1 channel, and this resulted in good predictions of experimental data. Kinetic details of spermine block were calculated using the "Q-matrix method," as described by Colquhoun and Hawkes (1995). Matrix Q was constructed such that each element (i,j) was equal to the rate constant from state i to state j, and each element (i,i) was set to be equal to the negative sum of all other elements in row i. State occupancy at time t was calculated as $p(t) = p(0)e^{Qt}$, where $p(t)$ is a row vector containing one element corresponding to occupancy of each state in the model at time t. All tasks required for solving these equations were performed in MathCad 2000.

RESULTS

Spermine Blocks Kir2.1 D255X Mutant Channels

Upon examining the properties of spermine block in WT Kir2.1 and several D255 mutants in inside-out patches, several effects of these cytoplasmic domain mutations on the properties of spermine block were immediately apparent. With the exception of D255E, all cytoplasmic domain mutant channels exhibit considerable slowing of the blocking rate when compared with WT Kir2.1. As illustrated in Fig. 2, this effect is enormous in the D255R and D255K mutants, which (even at a 10-fold higher spermine concentration) exhibit essentially no block over the duration of a voltage pulse that results in complete block of WT Kir2.1 channels (Fig. 2, inset). Importantly, over much longer voltage pulses, D255R and D255K mutant channels are nevertheless substantially blocked by spermine, but with a more pronounced pedestal of sustained current (Fig. 2, and see below). The data indicate that the apparent loss of steady-state rectification of D255R channels that is observed during brief voltage steps (Pegan et al., 2005) is actually due to extreme slowing of the spermine blocking rate. D255A channels also exhibited slower spermine block, with kinetics intermediate between those of WT Kir2.1 and D255R/K channels. The consistent effects of negative versus positive charge substitutions indicate that the observed effects on spermine blocking rate

Published July 16, 2007

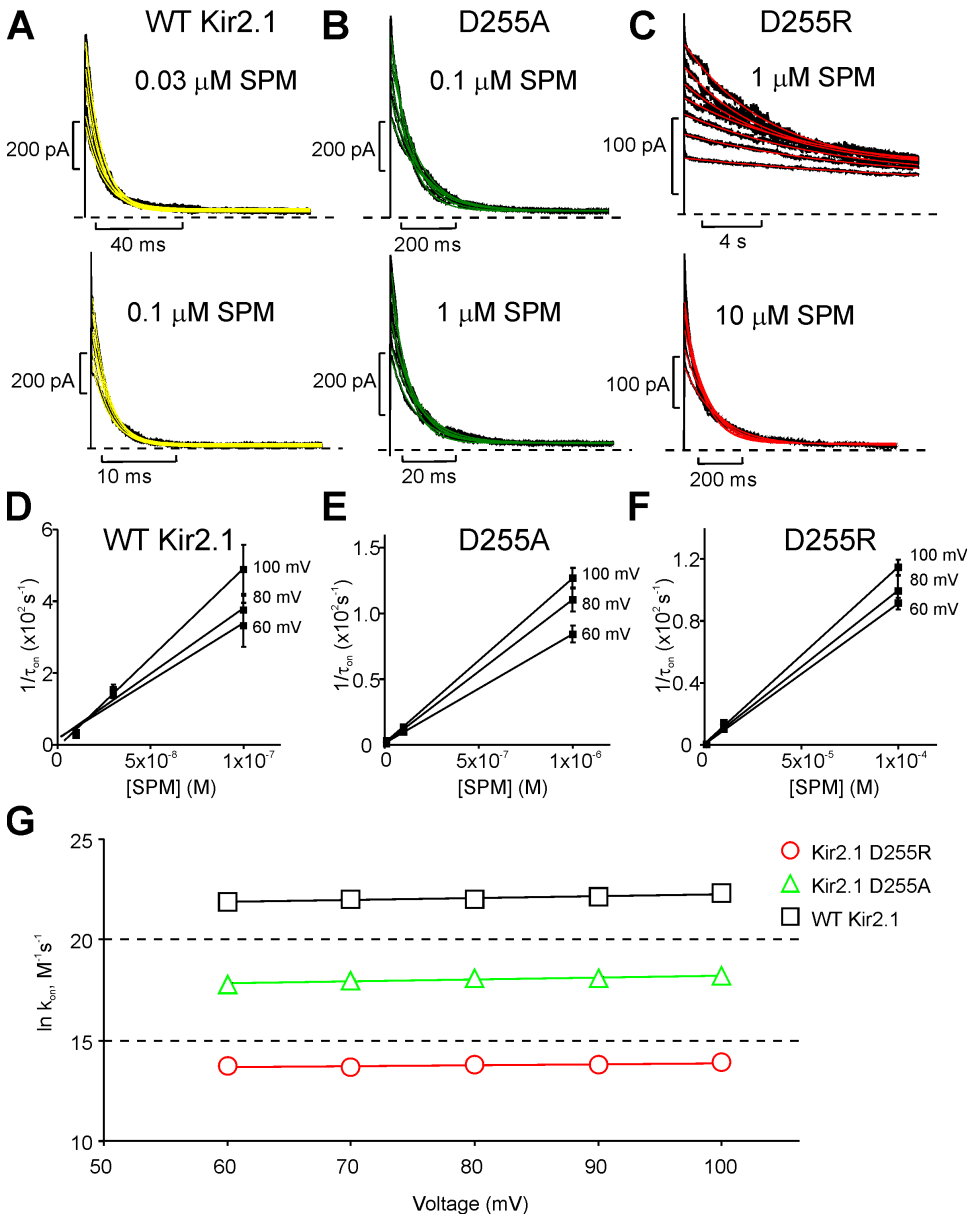

Figure 4. Determination of microscopic blocking rates in WT Kir2.1 and D255 mutants. (A–C) Representative currents in response to positive voltage steps for WT Kir2.1, D255A, and D255R channels at multiple spermine concentrations and voltages, fit to a single exponential decay equation. (D–F) Derived blocking time constants were extrapolated to determine the 0 mV blocking rate and the associated valence of block. (G) Blocking rate constant versus voltage for WT and mutant channels. In each channel, the blocking rate is very weakly dependent on voltage (very shallow slope of the fit lines), but the magnitude of the blocking rate constant varies dramatically between mutants.

depend on the charge at this position, and are not a nonspecific structural disruption of the mutations.

Steady-State Properties of Spermine Block of Kir2.1 and Cytoplasmic Domain Mutants

These initial observations, slower kinetics and more pronounced sustained currents in D255 mutants, are reflected in the steady-state blockade properties of these channels over a range of voltages and spermine concentrations (Fig. 3). At a low concentration of spermine (0.1 μM), plots of relative conductance (Grel) vs. voltage for WT Kir2.1 and the D255A mutant nearly overlap (Fig. 3, A–C), with a slightly larger Grel (reflecting a larger sustained current) in D255A channels at positive voltages. In 0.1 μM spermine (at +80 mV), the sustained current is ~3% ($n = 9$) of control current in WT Kir2.1 channels, and 6% ($n = 5$) of control current in D255A channels (Fig. 3 C).

Examination of spermine blockade in D255R channels at low spermine concentrations was impractical, due to the very slow kinetics of block in this mutant (Fig. 2). However, at higher (10–100 μM) spermine concentrations, where the kinetics of blockade in D255R are more amenable, it is apparent that WT Kir2.1, D255A, and D255R are all blocked by spermine with quite similar voltage dependence and potency but with other important differences in steady-state Grel- voltage plots (Fig. 3, D–F). First, at high spermine concentrations, WT Kir2.1 exhibits a weakly voltage-dependent shallow phase of spermine block at negative voltages. This feature likely results from spermine binding to a low affinity site in the cytoplasmic domain of the channel

Published July 16, 2007

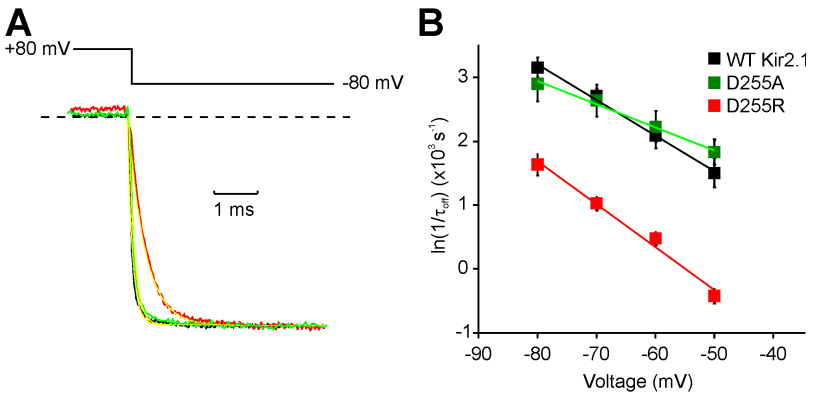

Figure 5. Spermine unblocking rates in WT Kir2.1, D255A, and D255R channels. (A) Representative current traces in response to a hyperpolarizing step to −80 mV in WT Kir2.1 (black), D255A (green), and D255R (red); monoexponential fits are superimposed in yellow. Before the hyperpolarizing pulse, channels were blocked in 10 μM spermine with voltage pulses to +80 mV. (B) Unblocking time constants were determined over a range of voltages and extrapolated to 0 mV by linear regression. Spermine unblock shows similar voltage dependence in all three channels examined, and a modestly slower rate in D255R channels relative to D255A or WT Kir2.1.

(Xie et al., 2002; Shin and Lu, 2005). The D255A and D255R mutations essentially abolish this shallow component of the Grel-voltage relationship (Fig. 3 F), in agreement with a previous characterization of Kir2.1 D255A (Shin et al., 2005). An additional feature of D255R channels, that is absent or much less pronounced in WT Kir2.1 or D255A, is an intrinsic inward rectification in the absence of polyamines (Fig. 3 D). This intrinsic rectification is similar to the effects of mutating other negatively charged residues in the Kir2.1 cytoplasmic domain (Guo et al., 2003; Fujiwara and Kubo, 2006), or the M2 asparagine (N171R or N171H, at neutral or acidic pH) in ROMK1 (Lu and MacKinnon, 1994, 1995). Similar observations have also been made after neutralization of negatively charged residues near the entrance to the inner cavity of BK channels (Zhang et al., 2006) and presumably reflects electrostatic repulsion of outwardly directed K^+ ions.

Multiple quantitative studies of spermine block have demonstrated that models consisting of at least two sequential blocking steps are required to simulate the multiple components of the Grel-voltage plots in WT Kir2.1 channels (Lopatin et al., 1995; Xie et al., 2003; Shin and Lu, 2005). These sequential equilibria comprise an initial, weakly voltage-dependent, binding step likely at a shallow site in the Kir pore (near the cytoplasmic entrance of the channel), and subsequent movement of spermine toward a second deep binding site. The exact physical location of this second site has been debated (Guo and Lu, 2003; Guo et al., 2003; Kurata et al., 2004, 2006). Although effects on the shallow component of spermine block are clear in the D255A and D255R mutant channels, effects on the steeply voltage-dependent component of spermine block are much less evident, consistent with these mutations having little or no impact on the deep spermine binding site (see Discussion).

Mechanistic Basis for "Sustained" Current through Kir2.1

Recent characterizations of Kir2.1 and other Kir channels have indicated that spermine and other polyamines may permeate these channels, albeit at a very slow rate (Guo and Lu, 2000; Dibb et al., 2003; Makary et al., 2005). Here, we consider the possibility that the balance between the rate of spermine permeation to the external solution, and the rate of spermine entry from the cytoplasm, accounts for the sustained current at depolarized voltages. For example, in a channel with a very fast spermine blocking rate, spermine permeation would be rapidly followed by reentry of a second spermine molecule, and very little sustained current would be expected. By contrast, in a channel with a very slow spermine blocking rate, spermine bound to the second site could exit through the selectivity filter, leaving the channel unblocked and capable of sustaining a K^+ current, before entry of another spermine ion into the channel pore. By similar reasoning, the magnitude of the sustained current should also depend on the concentration of cytoplasmic spermine, which we observe (Fig. 3). Alternatively, the entry rate would increase at elevated concentrations of spermine in the cytoplasm, leading to a smaller sustained current. This basic mechanistic outline for the "sustained" current is explored in more detail later, using a kinetic model (see Discussion).

To determine the rate of spermine block for WT Kir2.1, D255A, and D255R channels, the time course of spermine block over a range of positive voltages and spermine concentrations were fit with a single exponential equation (Fig. 4). Overall, the voltage dependence of the blocking rate at positive voltages is very weak in both D255 mutants and WT Kir2.1 (Fig. 4 C), consistent with previous descriptions of the wild-type channel (Lopatin et al., 1995; Shin and Lu, 2005). However, as evident in data presented in Fig. 2, the blocking rates for spermine are smaller in D255A channels, and dramatically smaller in the D255R mutant. Spermine unblock from WT Kir2.1, D255A, and D255R could be well described by monoexponential fits, and exhibited similar voltage dependence in all three channels over the range of −80 to −50 mV. In contrast to the dramatic slowing of forward blocking rates, the D255R and D255A mutations produced only small effects on the unblocking rate (Fig. 5). Spermine unblock rates were comparable between WT Kir2.1 and D255A channels, and slightly slower (approximately fivefold) in D255R channels.

Published July 16, 2007

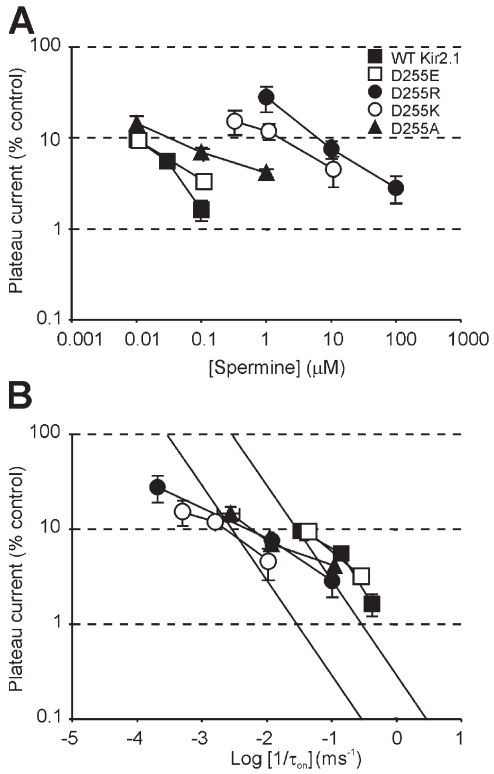

Figure 6. Relationship between on-rate and plateau current in WT Kir2.1 and the D255 mutants. (A) Plateau current versus spermine concentration at +80 mV, in WT Kir2.1, D255E, D255A, D255K, and D255R. In WT Kir2.1 and the D255 mutants, the magnitude of the plateau current depends on the cytoplasmic spermine concentration, although at any given concentration, the plateau current differs significantly between channel types. (B) Plateau current as a function of the blocking rate (log $[1/\tau_{on}]$) for WT Kir2.1, D255E D255A, D255K, and D255R. Across the WT and D255 mutant channels, the magnitude of the plateau current and the blocking rate are similarly related and fall upon a similar continuum. The solid lines are a prediction of the relationship between apparent spermine blocking rate ($1/\tau_{on}$) and the magnitude of the sustained current, based on the kinetic model described in Fig. 7 A, with a spermine permeation rate of 0.3 (leftmost line) or 3 s^{-1} (rightmost line). Model predictions were determined by simulating currents at +80 mV over a range of spermine concentrations and measuring the relevant parameters ($1/\tau_{on}$, and sustained current magnitude) from the simulated data.

To test the idea that the balance of spermine entry and spermine permeation underlies the sustained current observed in WT Kir2.1, we examined the quantitative relationship between the apparent spermine blocking rate ($1/\tau_{on}$) and the magnitude of the sustained current (Fig. 6). Even though the magnitude of sustained current varies substantially between the different channel constructs, in each case the sustained current increases as the spermine concentration is reduced (Fig. 6 A). When the data are replotted as a function of apparent spermine blocking rates in the different cytoplasmic domain mutants, the data for WT Kir2.1, and all of the D255 mutant channels, lie on approximately the same continuum

TABLE I

Model Parameters for Spermine Block of Kir2.1 and D255 Mutant Channels

	Rate			zδ
	WT Kir2.1	D255A	D255R	
O→B1	$1.725 \times 10^9\ M^{-1}s^{-1}$	$4.99 \times 10^7\ M^{-1}s^{-1}$	$5.8 \times 10^5\ M^{-1}s^{-1}$	0.23
B1→O	$1.03 \times 10^5\ s^{-1}$	$4.50 \times 10^4\ s^{-1}$	$2.82 \times 10^4\ s^{-1}$	0.19
B1→B2	$1.39 \times 10^4\ s^{-1}$	$9.97 \times 10^4\ s^{-1}$	$1.38 \times 10^6\ s^{-1}$	3.38
B2→B1	$2.77 \times 10^2\ s^{-1}$	$2.55 \times 10^2\ s^{-1}$	$54\ s^{-1}$	1.39
B2→O	$3.9\ s^{-1}$	$0.30\ s^{-1}$	$0.45\ s^{-1}$	0.01

(Fig. 6 B), demonstrating that the magnitude of the sustained current depends similarly on the spermine blocking rate (rather than the absolute spermine concentration) in each of the channels. This consistency suggests that it is indeed the balance of the spermine entry rate and the permeation rate that determines the magnitude of the sustained current, and moreover, that the spermine permeation rate is likely similar in WT Kir2.1 and the cytoplasmic domain mutants (see Discussion).

DISCUSSION

Strong inward rectification of Kir channels arises from steeply voltage-dependent block by polyamines (Nichols and Lopatin, 1997). This process requires movement of blocking spermine ions through the long Kir channel pore (Nishida and MacKinnon, 2002; Kuo et al., 2003; Pegan et al., 2005) to their most stable binding site, which appears to lie deep in the inner cavity, near the entrance to the selectivity filter (Kurata et al., 2006). Polyamine block comprises at least two sequentially related blocking steps that can be roughly correlated to structural features of the channel, specifically a series of negatively charged residues that line the Kir channel pore. A weakly voltage-dependent shallow blocking step involves interactions between spermine and several negatively charged residues in the cytoplasmic domain of the channel (D255, D259, E224, and E299). This is followed by a more strongly voltage-dependent step that depends critically on interactions between spermine and the rectification controller residue in the inner cavity (D172 in Kir2.1 channels). In this study, we have investigated the role of a recently identified residue in the Kir cytoplasmic domain (D255) in spermine block of Kir2.1. Our findings bolster a general model in which negatively charged residues in the cytoplasmic domain primarily regulate the kinetics of block, while having minor or indirect effects on the affinity of polyamines in their most stable deep blocked state.

Mutations of the D255 residue exert enormous effects on the overall forward blocking rate of spermine, with the apparent spermine on-rate slowed by nearly four orders of magnitude between the WT Kir2.1 channel and the D255R mutant (Figs. 2–4). However, with

Published July 16, 2007

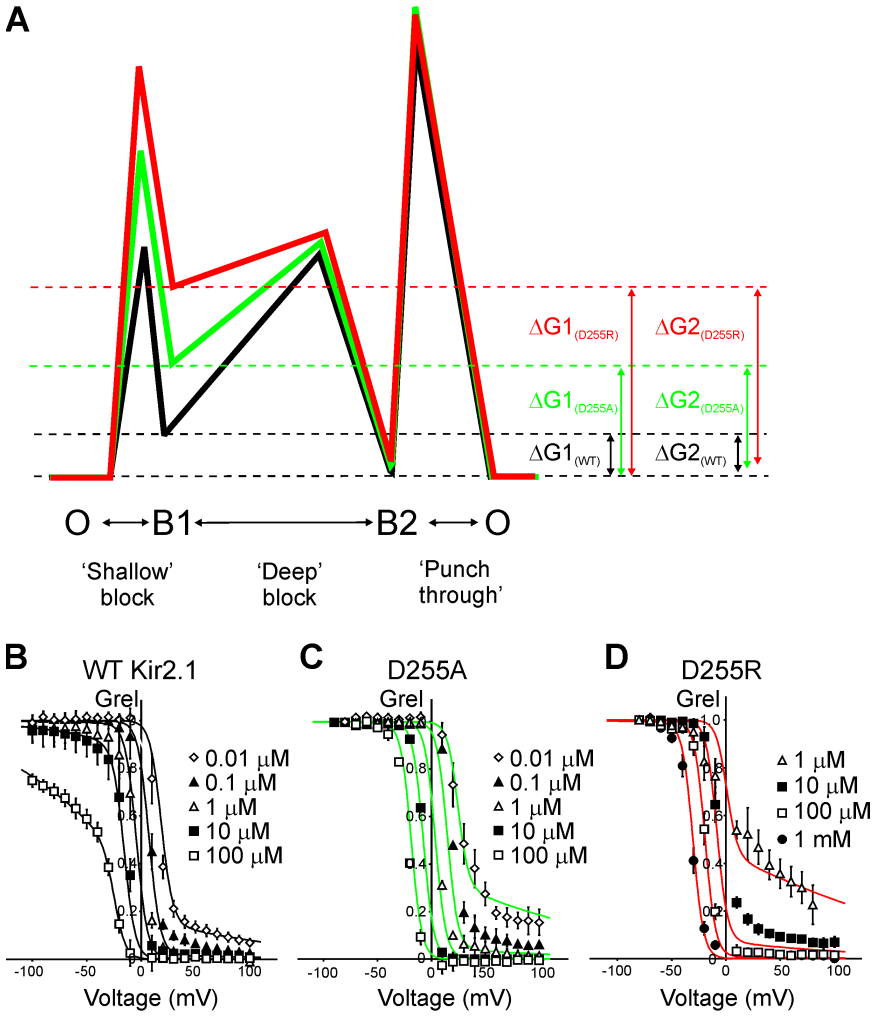

Figure 7. Kinetic model describing blockade by sequential binding and permeation of spermine in the Kir2.1 pore. The model comprises a weakly voltage-dependent shallow blocking equilibrium (O-B1), followed by a strongly voltage-dependent deep blocking equilibrium (B1-B2), followed by a permeation step that returns the channel to the open state (B2-O). Solid lines represent energy level diagrams for WT Kir2.1 (black), D255A (green), and D255R (red), illustrating the model manipulations required to reproduce the experimentally observed effects of mutations at residue D255. Transitions are scaled horizontally by voltage dependence, and vertically by potential energy. The predicted effects of the D255 mutations are localized almost entirely to the energy level of the B1 state, and the height of the O-B1 energy barrier. (B–D) Steady-state blockade properties are shown for (B) WT Kir2.1, (C) D255A, and (D) D255R channels in the presence of a range of spermine concentrations (between 1 mM and 0.01 μM). Fits to the data in each panel are the result of simultaneously fitting data at all characterized spermine concentrations with the kinetic model described in A (fitted parameters are listed in Table I).

sufficiently long depolarizing pulses, the mutant channels are blocked by spermine, suggesting that the affinity of spermine binding in its deep blocked state is essentially unaffected by D255 mutation (Shin et al., 2005). Grel-voltage curves describing steady-state spermine blockade are almost superimposable between WT Kir2.1 and the D255 mutant channels (Fig. 3, C and F) at mid-range voltages, the most significant differences being the appearance of a more prominent "plateau" conductance, and the loss of the shallow phase of block in the D255A/K/R mutant channels. The suggestion that this plateau current may be determined by relative rates of spermine block and spermine permeation through the selectivity filter is explored in more detail below with a kinetic model.

Kinetic Model of Spermine Block and Permeation

To investigate the relationship between the relative rates of spermine block and spermine permeation, we constructed a kinetic model describing interactions between spermine and Kir2.1 channels. The model is depicted as an energy level diagram in Fig. 7 A, with potential energy on the vertical axis and effective valence (i.e., voltage dependence) on the horizontal axis. Without assessing temperature dependence of spermine block, absolute energies cannot be derived for energy barriers in this scheme, although the relative energy levels of wells and barriers are appropriately scaled in Fig. 7 A. As in previous descriptions of Kir2.1 blockade by spermine and other compounds, the model comprises two sequential blocking steps (Lopatin et al., 1995; Shin and Lu, 2005). In addition, the model includes a permeation step, which is envisioned as deep blocked spermine permeating through the selectivity filter (Guo and Lu, 2000; Shin and Lu, 2005). The channel briefly remains open, permitting K^+ efflux and generating the sustained current. Spermine permeation as the physical basis for the observed sustained current is supported by earlier reports that philanthotoxin (spermine with a bulky adduct at one end of the chain) application abolishes sustained currents through Kir2.1 at depolarized voltages (Guo and Lu, 2000). Assuming that polyamine efflux is diluted infinitely in the extracellular solution, spermine entry from the extracellular side will be nonexistent, and we can derive an algebraic solution that predicts the steady-state proportion of channels that are blocked at any given

Published July 16, 2007

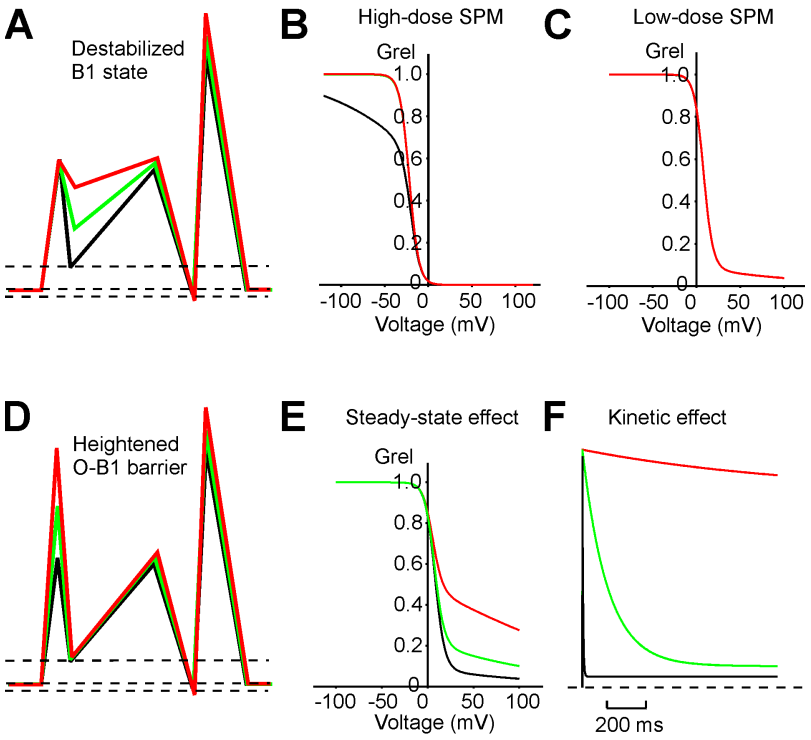

Figure 8. Effects of changing barrier heights and energy levels consistent with the effects of the D255A and D255R mutations. (A–C) Raising the B1 energy level abolishes the shallow phase of block at high spermine concentrations (B, black versus red), but has minimal effects at low spermine concentrations (C). (D–F) Raising the O-B1 energy barrier results in an enhanced plateau current at low spermine concentrations (E, steady-state effect) and slower kinetics of blockade (F, kinetic effect).

voltage or concentration of spermine. Solid lines included in plots of steady-state Grel vs. voltage (Fig. 7, B–D) are the predictions of this model (fitted parameters are illustrated visually in Fig. 7 A; for absolute fitted parameters of the kinetic model, see Table I).

We used experimental spermine blocking rates to constrain the voltage dependence and rate of the O→B1 transition. Although the model comprises multiple equilibria, at positive voltages and with the spermine concentrations used, O→B1 is essentially rate limiting, and so the derived k_{on} for spermine block (Fig. 4) was used to approximate the rate constant for the O→B1 transition. Spermine unblock in the model is determined predominantly by the B2→B1 transition, and was constrained by the measured rate and voltage dependence of spermine unblock (Fig. 5). As mentioned, the effects of D255 mutations on the spermine unblock rate were modest. This leaves six free parameters in the model including three rates, and three voltage-dependent terms. For simplicity, we fit the model initially to the WT Kir2.1 data, and used the fitted voltage dependences to constrain subsequent fits to data from D255A and D255R channels. In this way, only three free parameters were solved for the fits to D255A and D255R data (the B1→O rate, B1→B2 rate, and the B2→O spermine permeation rate).

Grel-voltage curves for WT Kir2.1 and the D255A and D255R mutants over a range of spermine concentrations are shown in Fig. 7 (B–D). The solid lines in Fig. 7 (B–D) are simultaneous fits of the model in Fig. 7 A, and reproduce major features of the experimental data over a wide range of concentrations and voltages. Important differences in the magnitude of sustained current in the WT Kir2.1 channel versus the D255 mutants are predicted; at the highest concentrations of spermine (~100 μM or higher), blockade of all three channels is essentially complete at positive voltages, but, in each case, a sustained current becomes apparent at positive voltages as the spermine concentration is reduced. The magnitude of the sustained current is greater in each of the D255 mutants, and particularly D255R, which continues to conduct ~10% of peak current even in 10 μM spermine (+80 mV, $n = 6$), and ~25% of peak current in 1 μM spermine (+80 mV, $n = 4$).

Blocker Permeation Accounts for Sustained Current through Kir2.1

The important outcome of the modeling is that properties of D255 mutant channels are predicted almost entirely by changes in (a) the height of the energy barrier for entry into the initial shallow blocked state (movement of a blocking ion from the cytoplasm into the channel pore), and (b) the blocker affinity of the shallow blocked state (Fig. 7 A). These two manipulations of the model reflect two distinct experimental features. The energy barrier between O and B1 is the prime determinant of the rate of blockade predicted by the model, and so elevation of this barrier (without altering the energy level of either O or B1) results in slower kinetics of block. This manipulation alone (Fig. 8, D–F) is insufficient to account for the loss of the shallow component of the steady-state Grel-voltage curves observed

Published July 16, 2007

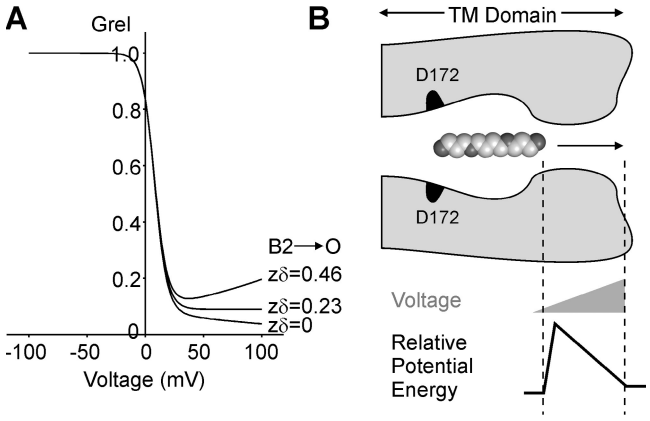

Figure 9. Model predictions of the effect of the voltage dependence of spermine permeation on steady-state blocking parameters. (A) The balance of spermine block and permeation determines the magnitude of the plateau current. Therefore, the respective voltage dependences of these two processes determine the shape of the Grel-voltage relationship at positive voltages. If the valence of permeation is smaller than the valence of block (0.23 for the O→B1 transition), the Grel-V relationship slopes downward at positive voltages. If the voltage dependence permeation is greater than the valence of the blocking transition, the Grel-V relationship turns upward at positive voltage (similar to what is observed in CNG channels, and contrary to what is observed in Kir2.1). (B) Potential physical interpretation of the apparent weak valence of spermine "punch through." A spermine ion is shown bound deep in the Kir channel, at its likely binding site as identified by blocker protection experiments (Kurata et al., 2006). If spermine traverses only a small fraction of the transmembrane field before reaching the transition state for the punch-through step, the apparent voltage dependence of the punch-through step will be accordingly small.

in D255 mutant channels. In the model, ablation of the weakly voltage-dependent component of spermine block requires destabilization of the B1 state (Fig. 8, A–C). The combination of these two manipulations then accounts for both the loss of shallow spermine block and the slower kinetics of spermine block observed in D255 mutant channels.

These straightforward predictions regarding the properties of spermine block also provide important insights regarding blocker permeation. As suggested earlier, a potential mechanistic explanation for the plateau conductance at depolarized voltages is that spermine is able to slowly permeate through the selectivity filter into the extracellular solution. In channels with a slow spermine blocking rate, there would be some delay between the exit of a blocking spermine into the extracellular solution, and the reentry of a second spermine ion from the intracellular side, during which K^+ ions could permeate the channel. Macroscopically, K^+ permeation during this delay would result in a sustained current, whose magnitude should grow smaller with either (a) increased intracellular spermine concentration or (b) in channels with an increased spermine entry rate. The presented kinetic model of spermine permeation and block is consistent with this general hypothesis for the mechanistic basic of sustained currents through Kir2.1. If a finite spermine permeation rate (B2→O) is included in the model, progressive elevation of the O-B1 energy barrier results in a progressively larger sustained current at positive voltages (Fig. 8, D and E), as does reduction of the intracellular spermine concentration. Although predictions of spermine permeation rates varied slightly between the D255 mutants and WT Kir2.1, modeled permeation rates between 0.4 and 4 s^{-1} recapitulate the experimental data over a wide range of spermine concentrations and voltages. These estimates are in reasonably good agreement with an earlier estimated spermine permeation rate of ~10 s^{-1} (Shin and Lu, 2005). The kinetic model also predicts a relationship between apparent spermine blocking rate (τ_{on}, as measured in Fig. 4) and sustained current magnitude (solid lines in Fig. 6 B, based on permeation rates of 0.3 and 3 s^{-1}). This predicted relationship is steeper than that observed experimentally, and we are unsure of the reasons for this shortcoming of the model in describing the data. Although the absolute relationship between blocking rate and sustained current is quite sensitive to changes in both the O→B1 transition and the spermine permeation rate (B2→O), the predicted slope of this relationship is a robust feature of the model and is not altered by even very large changes to individual rates. The discrepancy between model and data might reflect an overestimation of small plateau currents in our experiments, which are difficult to measure accurately and could potentially cause a "shallowing" of the relationship between blocking rate and sustained current.

An interesting feature of the kinetic model is that the magnitude of the sustained current at any given voltage is determined by the balance between the exit of spermine from the selectivity filter and entry from the cytoplasmic side of the channel. This highlights how a mutation near the cytoplasmic end of the pore, which affects blocker entry but makes no direct contribution to the deep blocking site, can nevertheless affect the overall block of the channel. We think of this phenomenon as a "long-pore" effect, in which mutations at one end of the pore can influence the apparent affinity of a permeant blocker by changing blocker throughput, but not blocker affinity in its most stable binding site.

Voltage Dependence of Spermine Permeation

The kinetic model predicts that, at positive voltages, the shape of the Grel-voltage curve depends strongly on the relative voltage dependence of the blocking (O→B1) and permeation (B2→O) steps. If the voltage dependences of these two transitions are perfectly matched, the sustained conductance remains constant as voltage is increased (Fig. 9 A, $z\delta = 0.23$). However, if the voltage dependence of the B2→O transition is smaller than the O→B1 transition, the Grel-voltage curve slopes downward

Published July 16, 2007

(Fig. 9 A, $z\delta = 0$, the case that most closely reproduces our experimental data). The opposite is true if the voltage dependence of permeation exceeds the voltage dependence of block (Fig. 9 A, $z\delta = 0.46$), as observed experimentally in spermine block of CNG channels (Lu and Ding, 1999; Guo and Lu, 2000).

The voltage dependence of the forward blocking rate can be experimentally constrained (Fig. 4) and, as mentioned above, is quite small ($\sim$0.25 elementary charges; Lopatin et al., 1995; Shin and Lu, 2005). The kinetic model predicts that the voltage dependence of permeation is even smaller, in order to reproduce the downward slope of the Grel-voltage curve at positive voltages (Fig. 7, B–D). What is the significance of such a small voltage dependence of the permeation step? One possible interpretation is that in reaching the deep blocked state (B2), spermine ions have already traversed almost all of the transmembrane electric field. Spermine is clearly able to protect residues between the rectification controller (D172 in Kir2.1) and the selectivity filter against MTSEA modification, implying a deep binding site in this region (Chang et al., 2003; Kurata et al., 2006) (see Fig. 9 B). However, most of the electric field is thought to drop across the selectivity filter, which makes it difficult to reconcile a blocking site below the filter with the suggestion that spermine in the B2 state has moved through most of the transmembrane field. In addition, other work has indicated that a significant fraction of the voltage dependence of spermine block of the shallow site (B1) and further progression into the deep site (B2) arises from coupled movement of permeant ions ahead of the blocker, suggesting that the blocking ion itself has not crossed most of the field while in the B2 state (Spassova and Lu, 1998; Shin et al., 2005).

A plausible interpretation of the observed weak voltage dependence of permeation is that blocker movement through most of the transmembrane field occurs after the energy barrier/transition state of the permeation step (Fig. 9 B). If movement from B2 to the transition state is associated with little charge movement through the field, the forward permeation rate will have weak voltage dependence (which could involve a small movement of the blocker itself and/or a coupled ion that remains in the selectivity filter when spermine is in the deep blocked state). Physically, this large energy barrier could be associated with entry of leading amines of spermine into the selectivity filter, although molecular modeling approaches suggest that spermine does not encounter a significant energy barrier until the leading amine reaches position S2 (Dibb et al., 2003). Another potential mechanism underlying this large initial energy barrier could be the loss of electrostatic stabilization by the negatively charged side chains at position D172 as spermine moves forward through the selectivity filter.

Conclusion

Neutralization or charge reversal of residue D255 causes dramatic slowing of the kinetics of spermine block in Kir2.1 channels, together with a sustained current at depolarized voltages. These data indicate that charged residues in the cytoplasmic domain exert critical control over the rate of spermine entry into the Kir pore. In addition, these effects of cytoplasmic pore mutations demonstrate a relationship between rates of blocker entry (from the cytoplasm) and blocker permeation (into the extracellular solution) in generating a sustained current through Kir2.1. Through a long-pore effect, mutations near the cytoplasmic entrance to the channel may alter the apparent affinity of permeant blockers such as spermine, not by changing blocker affinity in its stable binding site, but rather by changing the overall rate of blocker movement through the channel. Wild-type Kir2 channels appear to have evolved a mechanism for minimizing the plateau potential by ensuring a fast rate of polyamine block in the cytoplasmic domain.

This work was supported by National Institutes of Health grants HL54171 (to C.G. Nichols) and NS37682 (to P.A. Slesinger). H.T. Kurata is supported by a Canadian Institutes of Health Research Fellowship.

Lawrence G. Palmer served as editor.

Submitted: 8 January 2007
Accepted: 18 June 2007

REFERENCES

Chang, H.K., S.H. Yeh, and R.C. Shieh. 2003. The effects of spermine on the accessibility of residues in the M2 segment of Kir2.1 channels expressed in *Xenopus* oocytes. *J. Physiol.* 553:101–112.

Colquhoun, D., and A.G. Hawkes. 1995. A Q-matrix cookbook: how to write only one program to calculate the single channel and macroscopic predictions for any kinetic mechanism. *In* Single-Channel Recording. B. Sakmann and E. Neher, editors. Plenum Press, New York. 589–636.

Dibb, K.M., T. Rose, S.Y. Makary, T.W. Claydon, D. Enkvetchakul, R. Leach, C.G. Nichols, and M.R. Boyett. 2003. Molecular basis of ion selectivity, block, and rectification of the inward rectifier Kir3.1/Kir3.4 K^+ channel. *J. Biol. Chem.* 278:49537–49548.

Fakler, B., U. Brandle, E. Glowatzki, S. Weidemann, H.P. Zenner, and J.P. Ruppersberg. 1995. Strong voltage-dependent inward rectification of inward rectifier K^+ channels is caused by intracellular spermine. *Cell.* 80:149–154.

Fujiwara, Y., and Y. Kubo. 2006. Functional roles of charged amino acid residues on the wall of the cytoplasmic pore of Kir2.1. *J. Gen. Physiol.* 127:401–419.

Guo, D., and Z. Lu. 2000. Mechanism of IRK1 channel block by intracellular polyamines. *J. Gen. Physiol.* 115:799–814.

Guo, D., and Z. Lu. 2003. Interaction mechanisms between polyamines and IRK1 inward rectifier K^+ channels. *J. Gen. Physiol.* 122:485–500.

Guo, D., Y. Ramu, A.M. Klem, and Z. Lu. 2003. Mechanism of rectification in inward-rectifier K^+ channels. *J. Gen. Physiol.* 121:261–275.

Kubo, Y., and Y. Murata. 2001. Control of rectification and permeation by two distinct sites after the second transmembrane region in Kir2.1 K^+ channel. *J. Physiol.* 531:645–660.

Published July 16, 2007

Kuo, A., J.M. Gulbis, J.F. Antcliff, T. Rahman, E.D. Lowe, J. Zimmer, J. Cuthbertson, F.M. Ashcroft, T. Ezaki, and D.A. Doyle. 2003. Crystal structure of the potassium channel KirBac1.1 in the closed state. *Science.* 300:1922–1926.

Kurata, H.T., L.R. Phillips, T. Rose, G. Loussouarn, S. Herlitze, H. Fritzenschaft, D. Enkvetchakul, C.G. Nichols, and T. Baukrowitz. 2004. Molecular basis of inward rectification: polyamine interaction sites located by combined channel and ligand mutagenesis. *J. Gen. Physiol.* 124:541–554.

Kurata, H.T., L.J. Marton, and C.G. Nichols. 2006. The polyamine binding site in inward rectifier K^+ channels. *J. Gen. Physiol.* 127:467–480.

Lopatin, A.N., E.N. Makhina, and C.G. Nichols. 1994. Potassium channel block by cytoplasmic polyamines as the mechanism of intrinsic rectification. *Nature.* 372:366–369.

Lopatin, A.N., E.N. Makhina, and C.G. Nichols. 1995. The mechanism of inward rectification of potassium channels: "long-pore plugging" by cytoplasmic polyamines. *J. Gen. Physiol.* 106:923–955.

Lu, Z. 2004. Mechanism of rectification in inward-rectifier K^+ channels. *Annu. Rev. Physiol.* 66:103–129.

Lu, Z., and L. Ding. 1999. Blockade of a retinal cGMP-gated channel by polyamines. *J. Gen. Physiol.* 113:35–43.

Lu, Z., and R. MacKinnon. 1994. Electrostatic tuning of Mg^{2+} affinity in an inward-rectifier K^+ channel. *Nature.* 371:243–246.

Lu, Z., and R. MacKinnon. 1995. Probing a potassium channel pore with an engineered protonatable site. *Biochemistry.* 34:13133–13138.

Makary, S.M., T.W. Claydon, D. Enkvetchakul, C.G. Nichols, and M.R. Boyett. 2005. A difference in inward rectification and polyamine block and permeation between the Kir2.1 and Kir3.1/Kir3.4 K^+ channels. *J. Physiol.* 568:749–766.

Nichols, C.G., and A.N. Lopatin. 1997. Inward rectifier potassium channels. *Annu. Rev. Physiol.* 59:171–191.

Nishida, M., and R. MacKinnon. 2002. Structural basis of inward rectification: cytoplasmic pore of the G protein-gated inward rectifier GIRK1 at 1.8 Å resolution. *Cell.* 111:957–965.

Pegan, S., C. Arrabit, W. Zhou, W. Kwiatkowski, A. Collins, P.A. Slesinger, and S. Choe. 2005. Cytoplasmic domain structures of Kir2.1 and Kir3.1 show sites for modulating gating and rectification. *Nat. Neurosci.* 8:279–287.

Shin, H.G., and Z. Lu. 2005. Mechanism of the voltage sensitivity of IRK1 inward-rectifier K^+ channel block by the polyamine spermine. *J. Gen. Physiol.* 125:413–426.

Shin, H.G., Y. Xu, and Z. Lu. 2005. Evidence for sequential ion-binding loci along the inner pore of the IRK1 inward-rectifier K^+ channel. *J. Gen. Physiol.* 126:123–135.

Shyng, S., T. Ferrigni, and C.G. Nichols. 1997. Control of rectification and gating of cloned KATP channels by the Kir6.2 subunit. *J. Gen. Physiol.* 110:141–153.

Spassova, M., and Z. Lu. 1998. Coupled ion movement underlies rectification in an inward-rectifier K^+ channel. *J. Gen. Physiol.* 112:211–221.

Wible, B.A., M. Taglialatela, E. Ficker, and A.M. Brown. 1994. Gating of inwardly rectifying K^+ channels localized to a single negatively charged residue. *Nature.* 371:246–249.

Xie, L.H., S.A. John, and J.N. Weiss. 2002. Spermine block of the strong inward rectifier potassium channel Kir2.1: dual roles of surface charge screening and pore block. *J. Gen. Physiol.* 120:53–66.

Xie, L.H., S.A. John, and J.N. Weiss. 2003. Inward rectification by polyamines in mouse Kir2.1 channels: synergy between blocking components. *J. Physiol.* 550:67–82.

Xie, L.H., S.A. John, B. Ribalet, and J.N. Weiss. 2004. Regulation of gating by negative charges in the cytoplasmic pore in the Kir2.1 channel. *J. Physiol.* 561:159–168.

Yang, J., Y.N. Jan, and L.Y. Jan. 1995. Control of rectification and permeation by residues in two distinct domains in an inward rectifier K^+ channel. *Neuron.* 14:1047–1054.

Zhang, Y., X. Niu, T.I. Brelidze, and K.L. Magleby. 2006. Ring of negative charge in BK channels facilitates block by intracellular Mg^{2+} and polyamines through electrostatics. *J. Gen. Physiol.* 128:185–202.